Numerical analysis of the effects of tangential transpiration on the boundary layer characteristics

Received July 2001
Accepted August 2001

Burhan Çuhadaroğlu
Department of Mechanical Engineering, Karadeniz Technical University, Trabzon, Turkey

Keywords *Numerical methods, Boundary layers, Porous media*

Abstract *In the present study, the characteristics of the turbulent boundary layer developing on a porous wall with various angles of injection and suction are analyzed numerically with the proper boundary conditions. The finite difference method based on a control volume approach is used for solving the time averaged Navier-Stokes equations for incompressible flow in conjunction with the standard k-ε turbulence model equations. The wall functions of the viscous and turbulent sub-layers are modified to allow for the effect of the angle of injection and suction through the porous wall. A non-uniform staggered grid arrangement is used. The parameters studied include the velocity (V_w) and the angle (α) of the injection and suction. The present numerical results of the normal injection and suction are compared with the known experimental data and a good agreement is obtained. The numerical results also indicate that the characteristics of the turbulent boundary layer such as local friction coefficient, boundary layer thickness and shape factor are substantially influenced by the velocity and the angle of injection and suction.*

Nomenclature

C_f = local friction coefficient
C_μ, C_1, C_2, σ_k, σ_ε = turbulence model constants
G = generation rate of turbulent kinetic energy
H_{12} = shape factor, δ_1/δ_2
I,J = value at (i, j) cell
I_{MAX}, J_{MAX} = maximum values of grid numbers
k = turbulence kinetic energy
n = normal direction to the porous wall
p = pressure
Re = Reynolds number based on porous wall length, $U_\infty X_L/\nu$
r = mesh expansion ratio
S_ϕ = source term
Tu = turbulence intensity, $\mathrm{Tu} = 100\left[\frac{1}{3}(\overline{u'^2}+\overline{v'^2}+\overline{w'^2}\right]/U_\infty$
t = time
U_∞ = free-stream velocity
u_τ = friction velocity
u, v = velocity components
V_w = injection and suction velocity
X_L,Y_L = horizontal and vertical lengths of the computation domain
x, y = Cartesian coordinates

Greek symbols
α = angle of injection and suction
ε = turbulence energy dissipation rate
ΔX,ΔY = distances between the grid points
δ = boundary layer thickness
δ_1 = displacement thickness, $\delta_1 = \int_0^\delta (1-\frac{u}{U_\infty})dy$
δ_2 = momentum thickness, $\delta_2 = \int_0^\delta \frac{u}{U_\infty}(1-\frac{u}{\infty})dy$
κ = von Karman constant ($\kappa = 0.4$)
ϕ = any dependent variable (i.e. u, v, k, ε)

This work was funded by Karadeniz Technical University Research Fund.

International Journal of Numerical Methods for Heat & Fluid Flow, Vol. 11 No. 8, 2001, pp. 793-806.

Γ = coefficient of diffusion
μ = dynamic viscosity
ρ = density
υ = kinematic viscosity
τ = shear stress

Subscripts
eff = effective
p = intersection point
t = turbulent
w = wall

Superscripts
+ = normalized quantity
′ = fluctuating quantity
– = time average

Introduction

The study of turbulent boundary layer on a porous wall with injection and suction is of great importance for technological applications. Among them it may be mentioned that the introduction of a foreign gas into the boundary layer through a porous wall constitutes an effective film or transpiration cooling. This reduces the rate of heat transfer from the hot, streaming gas to the solid body, as is done for gas turbine blades. Similarly, this is a means of reducing the rate of heat flow from the boundary layer rendered very hot by kinetic heating on a body flying at a hypersonic velocity to its wall. Injection can also produce a considerable reduction in drag (see Schlichting, 1979).

Although the turbulent boundary layer on a porous wall with normal injection and suction has been studied by many investigators, the effects of the tangential injection and suction on the characteristics of boundary layer have not been studied in detail. Some experimental results of transpiration and film cooling through a porous wall were reviewed by Eckert and Drake (1972). An introductory review of boundary layers with normal suction and blowing was given by Schlichting (1979). The existing works on turbulent boundary layer, with and without normal transpiration, have been reviewed and also the skin-friction measurements at low Reynolds numbers with transpiration have been carried out by Simpson (1970). Schetz and Nerney (1977) experimentally investigated the turbulent boundary layer with normal injection and surface roughness. The results of this study reveal that the velocity and turbulence intensity in the turbulent boundary layer increased with increasing rate of injection. The effect of uniform normal mass bleed into the separated-reattaching flow over a backstep has been investigated experimentally by Yang *et al.* (1994). The flow over a backward-facing step with uniform normal mass bleed has been numerically analyzed by Yang and Kuo (1997) and the results obtained have been compared with the experimental data of Yang *et al.* (1994). The majority of the analysis of boundary layers developing on porous walls so far is limited to experiments and theories, whereas the numerical analysis of such flows gives more detailed information on the interrelationship between the boundary layer characteristics and porous wall parameters such as angle of injection.

Numerical studies of the prediction of turbulent boundary layer characteristics need to be formulated in the region close to the wall where the high velocity gradients are encountered. As is known, the turbulent boundary layer has sub-layers, e.g. the linear sub-layer, buffer zone, turbulent sub-layer (log-law region) and outer layer, which are represented by the wall functions. When the wall is

porous, the wall functions are modified to include the effect of injection or suction. Here, the numerical study of the effects of a uniform injection and suction with various angles through a porous wall on the turbulent boundary layer characteristics is presented. The numerical results of uniform normal injection are compared with the experimental data given by Schlichting (1979) and the agreement is found to be satisfactory.

Mathematical formulation

The governing equations

The time averaged Navier-Stokes equations incorporating the Boussinesq turbulent viscosity concept are used in conjunction with the turbulent viscosity defined by the high-Reynolds number version of the k-ε model of turbulence (see Launder and Spalding, 1979). The steady conservation equations for two-dimensional incompressible turbulent flow can be written as:

$$\frac{\partial}{\partial \mathrm{x}}(\rho \mathrm{u}\phi) + \frac{\partial}{\partial \mathrm{x}}(\rho \mathrm{v}\phi) = \frac{\partial}{\partial \mathrm{x}}(\Gamma \frac{\partial \phi}{\partial \mathrm{x}}) + \frac{\partial}{\partial \mathrm{y}}(\Gamma \frac{\partial \phi}{\partial \mathrm{y}}) + \mathrm{S}_\phi \qquad (1)$$

where ϕ represents any of the variables (u,v,k,ε) and S_ϕ is the corresponding source term. All the governing equations and constants used in this study are summarized in Table I.

Boundary conditions

At the inflow boundary of the computation domain uniform velocity profile imposed with:

$$\mathrm{u} = \mathrm{U}_\infty, \mathrm{k} = 1.5(\mathrm{Tu}.\mathrm{U}_\infty)^2, \varepsilon = \mathrm{C}_\mu^{3/4}\mathrm{k}^{3/2}/\kappa \mathrm{y}. \qquad (2)$$

Along the outflow and free boundaries where the flow field is regarded as fully developed, the normal derivatives of all properties are zero, i.e.:

Equation	ϕ	Γ	$\mathbf{S}_\phi$
Continuity	1	0	0
x-momentum	u	$\mathrm{u}_{\mathrm{eff}}$	$-\frac{\partial \mathrm{p}}{\partial \mathrm{x}} - \frac{\partial}{\partial \mathrm{x}}(\frac{2}{3}\rho \mathrm{k}) + \frac{\partial}{\partial \mathrm{x}}(\mu_{\mathrm{eff}}\frac{\partial \mathrm{u}}{\partial \mathrm{x}}) + \frac{\partial}{\partial \mathrm{y}}(\mu_{\mathrm{eff}}\frac{\partial \mathrm{v}}{\partial \mathrm{x}})$
y-momentum	v	μ_{eff}	$-\frac{\partial \mathrm{p}}{\partial \mathrm{y}} - \frac{\partial}{\partial \mathrm{y}}(\frac{2}{3}\rho \mathrm{k}) + \frac{\partial}{\partial \mathrm{x}}(\mu_{\mathrm{eff}}\frac{\partial \mathrm{u}}{\partial \mathrm{y}}) + \frac{\partial}{\partial \mathrm{y}}(\mu_{\mathrm{eff}}\frac{\partial \mathrm{v}}{\partial \mathrm{y}})$
Turbulence kinetic energy	k	$\frac{\mu_{\mathrm{eff}}}{\sigma_{\mathrm{k}}}$	$\mathrm{G} - \rho\varepsilon$
Turbulence energy dissipation rate	ε	$\frac{\mu_{\mathrm{eff}}}{\sigma_\varepsilon}$	$\frac{\varepsilon}{\mathrm{k}}(\mathrm{C}_1\mathrm{G} - \mathrm{C}_2\rho\varepsilon)$

Notes: $\mu_{\mathrm{eff}} = \mu + \mu_{\mathrm{t}}, \quad \mu_{\mathrm{t}} = \rho \mathrm{C}_\mu \mathrm{k}^2/\varepsilon$

$\mathrm{C}_\mu = 0.09, \ \mathrm{C}_1 = 1.44, \ \mathrm{C}_2 = 1.92, \ \sigma_{\mathrm{k}} = 1.0, \ \sigma_\varepsilon = 1.3$

$\mathrm{G} = \mu_{\mathrm{t}}\left\{\left[2(\frac{\partial \mathrm{u}}{\partial \mathrm{x}})^2 + 2(\frac{\partial \mathrm{v}}{\partial \mathrm{y}})^2\right] + \left[(\frac{\partial \mathrm{u}}{\partial \mathrm{y}}) + (\frac{\partial \mathrm{v}}{\partial \mathrm{x}})\right]^2\right\}$

Table I. Summary of equations solved

$$\frac{\partial u}{\partial n} = 0, \frac{\partial v}{\partial n} = 0, \frac{\partial k}{\partial n} = 0, \frac{\partial \varepsilon}{\partial n} = 0. \tag{3}$$

In order to obtain the wall functions in the near-porous wall region, the momentum equation of two-dimensional incompressible turbulent boundary layer with zero pressure gradient can be regarded, which is represented by (see Schlichting, 1979):

$$u\frac{\partial u}{\partial x} + v\frac{\partial u}{\partial y} = \frac{\partial}{\partial y}(\nu\frac{\partial u}{\partial y} - \overline{u'v'}). \tag{4}$$

Close to the wall, the derivative of $\partial u/\partial x$ is small and can be neglected (see Cebeci and Smith, 1974), the momentum equation then becomes:

$$v\frac{du}{dy} = \frac{d}{dy}(\nu\frac{du}{dy} - \overline{u'v'}). \tag{5}$$

Integrating equation (5) from y = 0 to any y and the using the porous wall conditions with tangential injection; $u(0) = V_w \cos\alpha$, $\nu(du/dy)|_{y=0} = \tau w/\rho = u_\tau^2$ and $\overline{u'v'}|_{y=0}$ at y = 0 (Figure 1) yields:

$$u_\tau^2 = \frac{\tau_t}{\rho} + \nu\frac{du}{dy} - (u - V_w\cos\alpha)V_w\sin\alpha \tag{6}$$

where $\tau_t/\rho = -\overline{u'v'}$.

The use of Prandtl's mixing-length expression with the mixing length formula described by van Driest (see Schlichting, 1979) gives:

$$\frac{\tau_t}{\rho} = (\kappa y)^2\left[1 - \exp(-\frac{yu_\tau}{\nu A})\right]^2(\frac{du}{dy})^2 \tag{7}$$

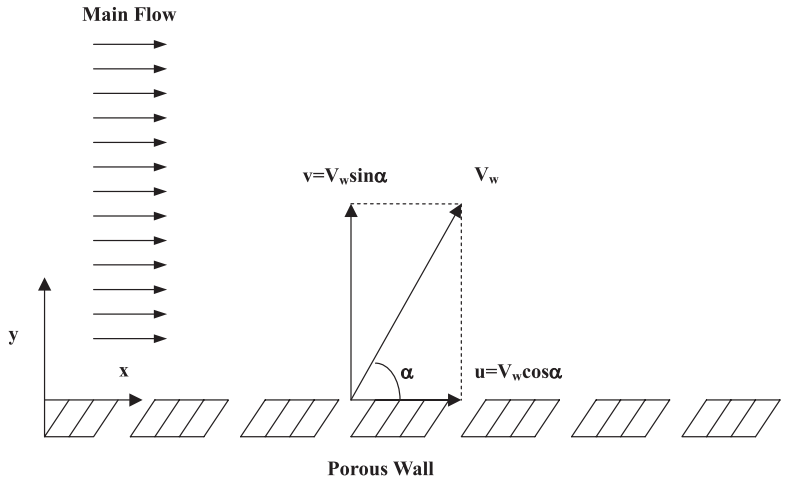

Figure 1.
The schematic representation of the flow field

where A is a damping-length constant, for which the best correct choice is about $A = 26 \exp(-5.9V_w/u_\tau)$ (see Cebeci and Bradshaw, 1977). Combining the equations (6) and (7) gives:

$$a(y)\left(\frac{du}{dy}\right)^2 + \nu\frac{du}{dy} - u_\tau^2 - (u - V_w\cos\alpha)V_w\sin\alpha = 0 \tag{8}$$

or,

$$\frac{du}{dy} = \frac{-\nu + \sqrt{\nu^2 + 4a(y)\left[u_\tau^2 + (u - V_w\cos\alpha)V_w\sin\alpha\right]}}{2a(y)} \tag{9}$$

where $a(y) = (\kappa y)^2\lfloor 1 - \exp(-yu_\tau/\nu A)^2\rfloor$. Multiplication of both numerator and denominator of equation (9) by $\nu + \sqrt{\nu^2 + 4a(y)[u_\tau^2 + (u - V_w\cos\alpha)V_w\sin\alpha]}$ yields:

$$\frac{du}{dy} = \frac{2\lfloor u_\tau^2 + uV_w\sin\alpha - (V_w^2\sin 2\alpha)/2\rfloor}{\nu + \sqrt{\nu^2 + 4a(y)\left[u_\tau^2 + uV_w\sin\alpha - (V_w^2\sin 2\alpha)/2\right]}}. \tag{10}$$

In terms of normalized quantities this equation can be written as:

$$\frac{du^+}{dy^+} = \frac{2\lfloor 1 + u^+V_w^+\sin\alpha - (V_w^{+2}\sin 2\alpha)/2\rfloor}{1 + \sqrt{1 + 4a(y^+)\left[1 + u^+V_w^+\sin\alpha - (V_w^{+2}\sin 2\alpha)/2\right]}} \tag{11}$$

where the normalized quantities are defined as:

$$u^+ = \frac{u}{u_\tau},\ y^+ = \frac{yu_\tau}{\nu},\ v_w^+ = \frac{v_w}{u_\tau},\ a(y^+) = (\kappa y^+)^2\left[1 - \exp(-\frac{y^+}{A})\right]^2. \tag{12}$$

Equation (11) defines the velocity gradient in the turbulent boundary layer. In the viscous sub-layer, neglecting the turbulent stress, i.e. taking $a(y^+) = 0$ in equation (11) and integrating it from the wall to an arbitrary non-dimensional coordinate with the condition of $u^+ = V_w^+\cos\alpha$ at $y^+ = 0$ gives:

$$u^+ = \frac{\exp(y^+V_w^+\sin\alpha) + (V_w^{+2}\sin 2\alpha)/2 - 1}{V_w^+\sin\alpha} \tag{13}$$

In the turbulent sub-layer, regarding the fact that, at large distances from the wall (i.e. outside the viscous sub-layer), it is possible to neglect the viscous stresses and taking $a(y^+) = (\kappa y^+)^2$ in equation (11) the relation for the velocity gradient is obtained as:

$$\frac{du^+}{dy^+} = \frac{\sqrt{1 + u^+V_w^+\sin\alpha - (V_w^{+2}\sin 2\alpha)/2}}{\kappa y^+} \tag{14}$$

The integration of Equation (14) from the point "p", at which the viscous sub-layer and turbulent sub-layer intersect to any y^+ gives:

$$u^+ = \frac{V_w^+ \sin\alpha}{4\kappa^2}\left[\ln\left|\frac{y^+}{y_p^+}\right|\right]^2 + \frac{1}{\kappa}\ln\left|\frac{y^+}{y_p^+}\right|\left[1 + u_p^+ V_w^+ \sin\alpha - (V_w^{+^2}\sin 2\alpha)/2\right]^{1/2} + u_p^+ \tag{15}$$

where u_p^+, y_p^+ and κ are functions of V_w^+ and Re_{δ_2} in general (see Simpson, 1970). For $V_w^+ = 0$, equation (15) reduces to the universal velocity distribution formula on a nonporous wall:

$$u^+ = \frac{1}{\kappa}\ln\left|\frac{y^+}{y_p^+}\right| + u_p^+ \tag{16}$$

In the case of normal injection ($\alpha = 900^\circ$), different investigators have evaluated u_p^+ theoretically as different functions of V_w^+, depending upon whose experimental results they were attempting to fit. Simpson (1970) criticized the results of the several investigators in conjunction with his experimental results and concluded that in normal injection, using the unblown constants $u_p^+ = 11$ and $\kappa = 0.4$, which seems to fit the low Reynolds number unblown data as a whole, y_p^+ is substantially independent of V_w^+. Finally, the wall functions used in this study with the constants of $u_p^+ = y_p^+ = 11.5$ and $\kappa = 0.4$ can be summarized as follows:

$$u^+ = \left\{ \begin{array}{llll} \text{Equation} & (13); & \text{for} & y^+ < y_p^+ \\ \text{Equation} & (15); & \text{for} & y^+ \geq y_p^+ \end{array} \right\}. \tag{17}$$

In the vicinity of the wall, the turbulent sublayer is in local equilibrium so that the rate of turbulence kinetic energy production is exactly equal to its dissipation rate ($G = \rho\varepsilon$). Therefore, at the point close to the porous wall, the value of turbulence kinetic energy k is calculated solving the transport equation of turbulence kinetic energy neglecting the production and dissipation terms, while the energy dissipation ε can be evaluated by the expression:

$$\varepsilon = \frac{C_\mu^{3/4} k^{3/2}}{\kappa y}. \tag{18}$$

Method of solution

The method of numerical solution used in the present study is based on solving the set of discretization equations iteratively using a point by point method. The discretization equations are derived by integrating the differential equations over a defined control volume. As is done in general, the calculation domain is discretized with a staggered grid which allows the prediction of the velocity components in the momentum grid points with the QUICK scheme,

while the other variables such as turbulence, kinetic energy, etc. are predicted in the basic grid points with the HYBRID scheme (see Patankar, 1980). At the end of each iteration, the pressure was computed and the velocity components are corrected satisfying the continuity equation, using the Marker and Cell Method (see Hirt and Cook, 1972).

The grid spacing in the normal direction (y) was arranged as non-uniform which has high-density grid points near the porous wall according to the distance formulae $\Delta Y_j = \Delta Y_{min}.r^{j-1} (\Delta Y_{min} = 0.001m, j = 1, 2, \ldots, J_{MAX})$. Where r is the mesh expansion ratio obtained through the iterative solution of $r = [(r-1)(Y_L/\Delta Y_{min})+1]_{1/JMAX}$. The uniform grid spacing was considered in the x direction with the distance formulae $\Delta X = X_L/I_{MAX}$ as seen in Figure 2. Based on a grid independence study, a 200 × 50 grid size was used in the calculating domain. The iterative solution of the discretization equations is considered to be converged when the normalized residuals of the equations are less than a prescribed value of 0.001. All computations were conducted on a PC – a 600Mhz-Pentium III computer.

Results and discussion

The problem analyzed corresponds to a Reynolds number ($Re = U_\infty X_L/(\nu)$ of 2×10^6 to allow the developing of the turbulent boundary layer. As is known well, in the boundary layer on a flat plate without injection and suction, transition from laminar to turbulent flow occurs at a critical level of Reynolds number of 3.5×10^5 to 10^6 (see Schlichting, 1979), depending on the turbulence intensity (Tu) of the free stream, i.e. it was of the order of 0.01 which was used as an inlet parameter in the present study.

A comparison of the normalized mean horizontal velocity profiles with various values of normalized injection and suction velocities is shown in Figure 3. It indicates that the predictions are seen to be in good agreement with the experiments. Streamlines of the flow field for different injection and suction velocities are plotted in Figure 4.

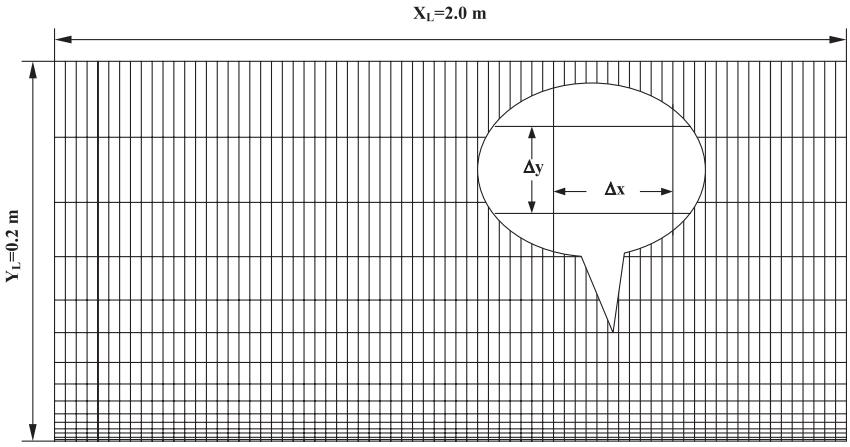

Figure 2.
The finite difference grid used in the finite difference solution

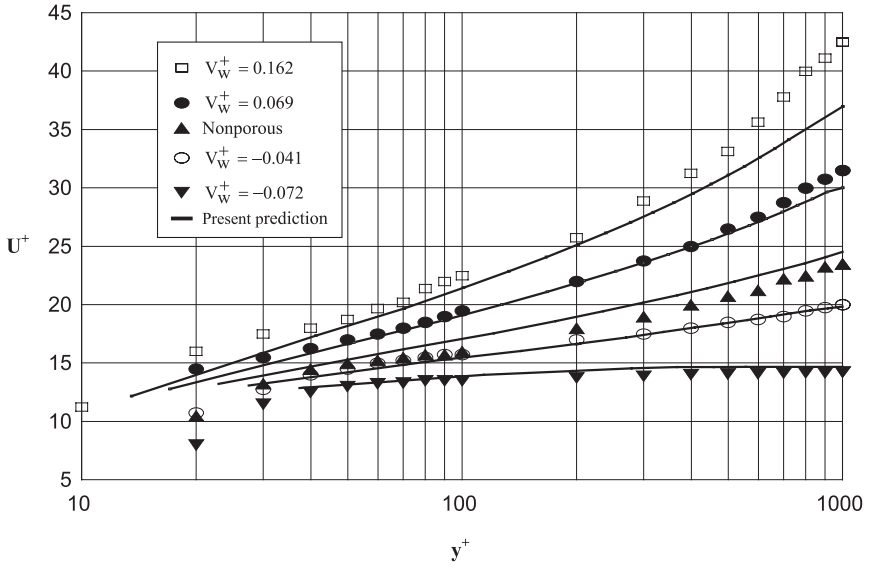

Figure 3.
Comparison of the normalized mean horizontal velocity profiles with the experimental data given by Schlichting (1979) for normal injection and suction

The effects of the angle of injection and suction through the porous wall on normalized mean horizontal velocity are shown in Figures 5 and 6. It can be seen clearly that the velocity profiles tend to be less steep, as the angle of injection increases from 1° to 180°. In the case of suction, increasing angle of suction from 1° to 180° causes the steeper velocity profiles. The velocity profiles are slightly affected by the angles from 1° to 90° and also from 150° and 180° of injection and suction, while the profiles are substantially affected by the angles from 90° to 150° in cases both of injection and suction.

The effects of the angle of the injection and suction on local friction coefficient, which is defined as:

$$C_f = \frac{2u_\tau^2}{U_\infty^2} \tag{19}$$

are depicted in Figures 7 and 8. It can be seen clearly that along the porous wall the local friction coefficient is increased with increasing angle of injection, while it is decreased with increasing angle of suction. It should also be mentioned here that the effect of the angles higher than 90° on the local coefficient variation is more considerable than the angles less than 90° in cases both of injection and suction.

Figure 9 shows that the rate of boundary layer thickness growth in the downstream direction decreases as the angle of injection increases. As is seen, while the boundary layer thickness growth significantly depends on the angle of injection for the values between 90° and 150°, the effects of the angles from 1° to 90° and also from 150° to 180° on the boundary layer

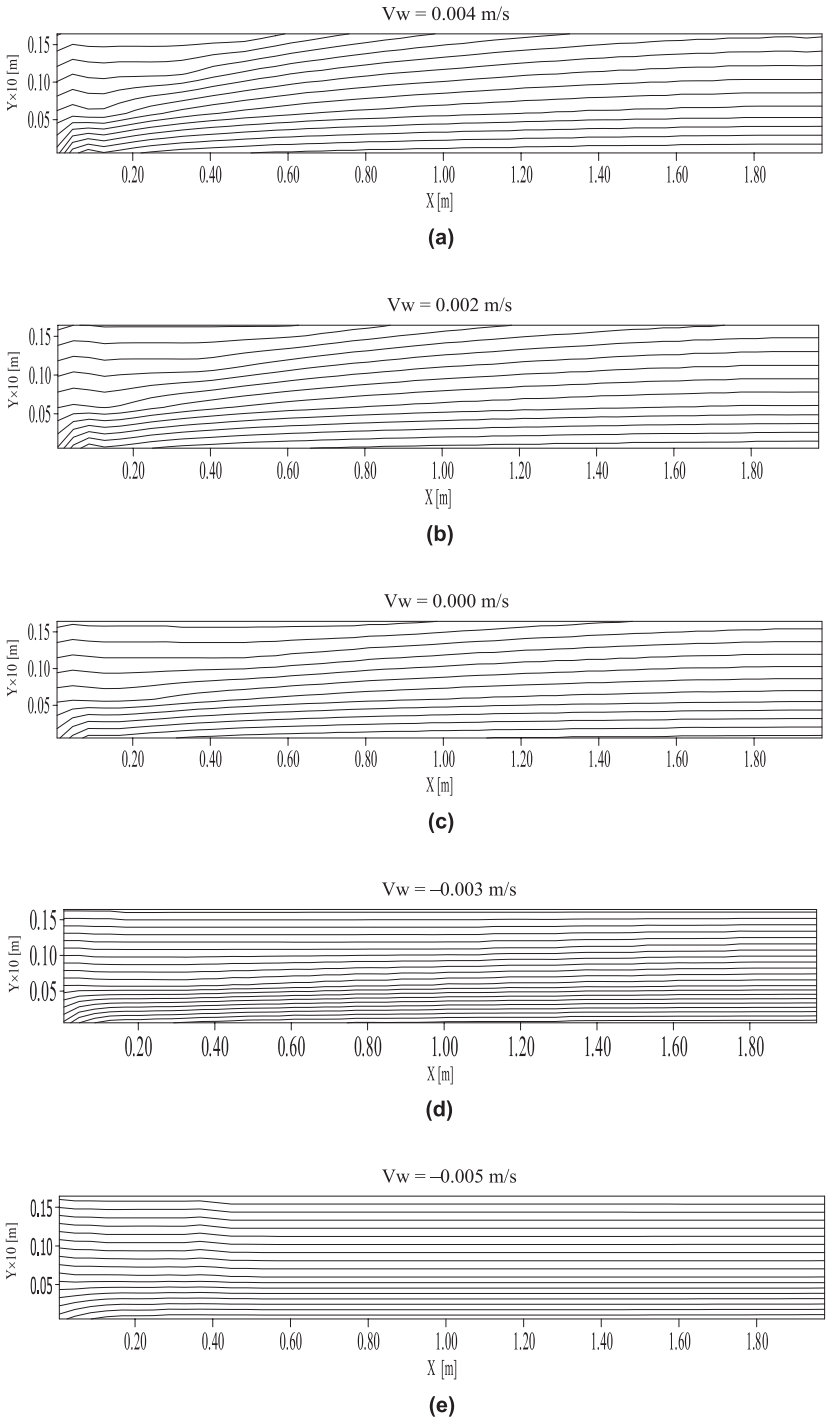

Figure 4.
The streamlines at different velocities of the normal injection and suction

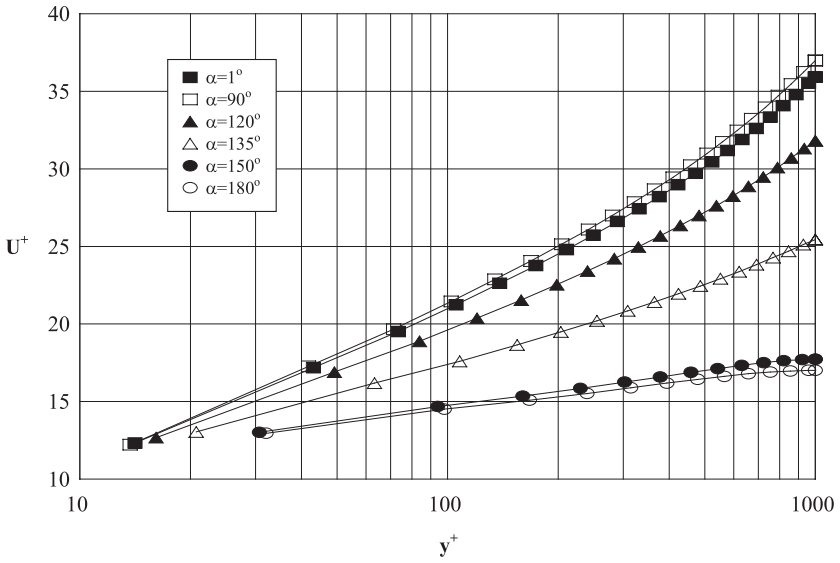

Figure 5.
Normalized mean horizontal velocity profiles at different angles of injection for V_w = 0.004 m/s

thickness growth can be regarded as unimportant. The effect of the tangential suction through the porous wall on the growth of the boundary layer thickness is also seen in Figure 10. Comparing the Figures 9 and 10, it can be seen that the boundary layer thickness variations in the downstream direction are quantitatively similar for the cases of injection with the angles of $1^\circ \leq \alpha \leq 90^\circ$ and suction with the angles of $150^\circ \leq \alpha \leq 180^\circ$.

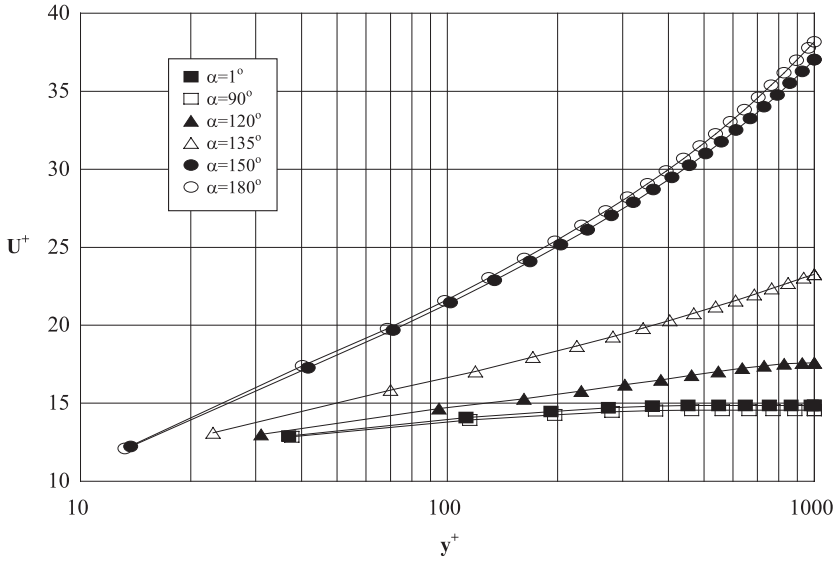

Figure 6.
Normalized mean horizontal velocity profiles at different angles of suction of V_w = –0.005 m/s

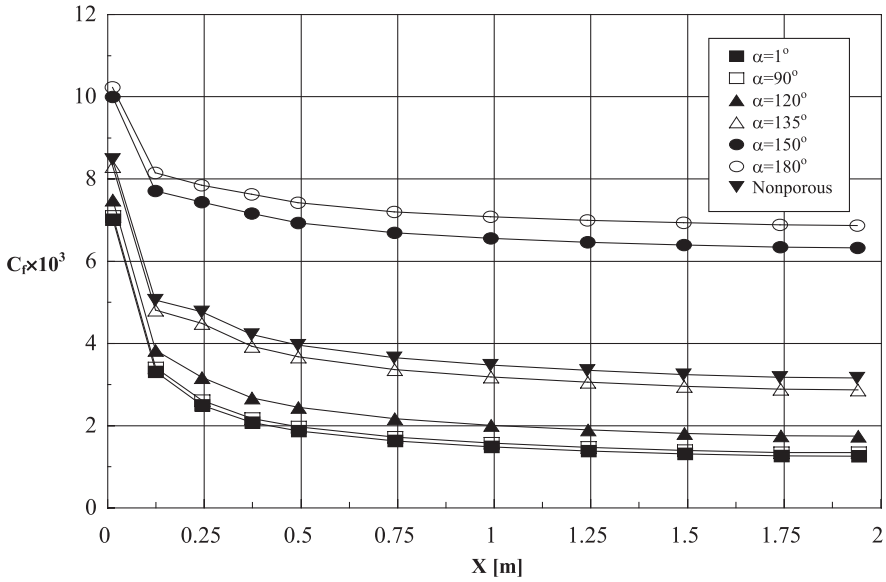

Figure 7.
Variation of the local friction coefficient along the wall at different angles of injection for V_w = 0.004 m/s

Another boundary layer characteristic is the shape factor defined as:

$$H_{12} = \frac{\delta_1}{\delta_2} \tag{20}$$

which is a good indicator of pressure gradient. The higher the H the stronger adverse pressure gradient and separation occurs at the certain values of the H.

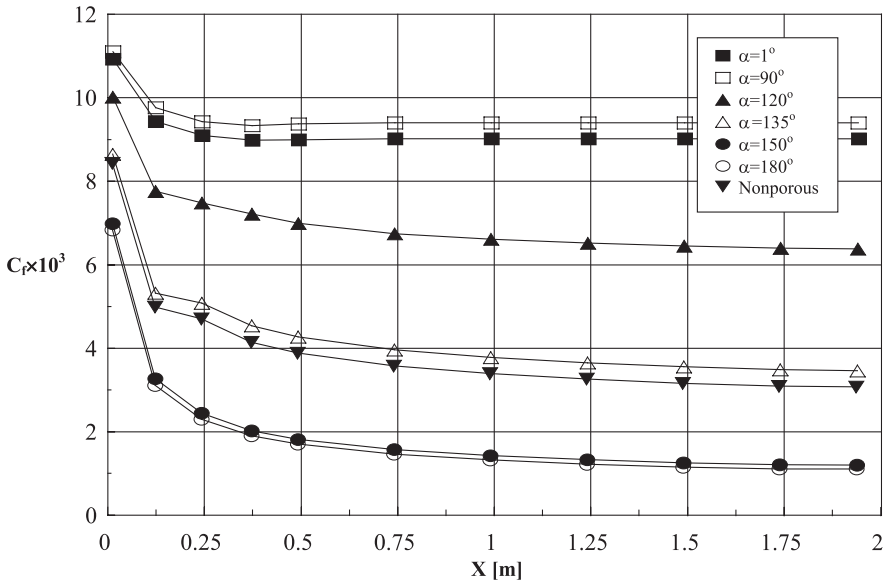

Figure 8.
Variation of the local friction coefficient along the wall at different angles of suction for V_w = –0.005 m/s

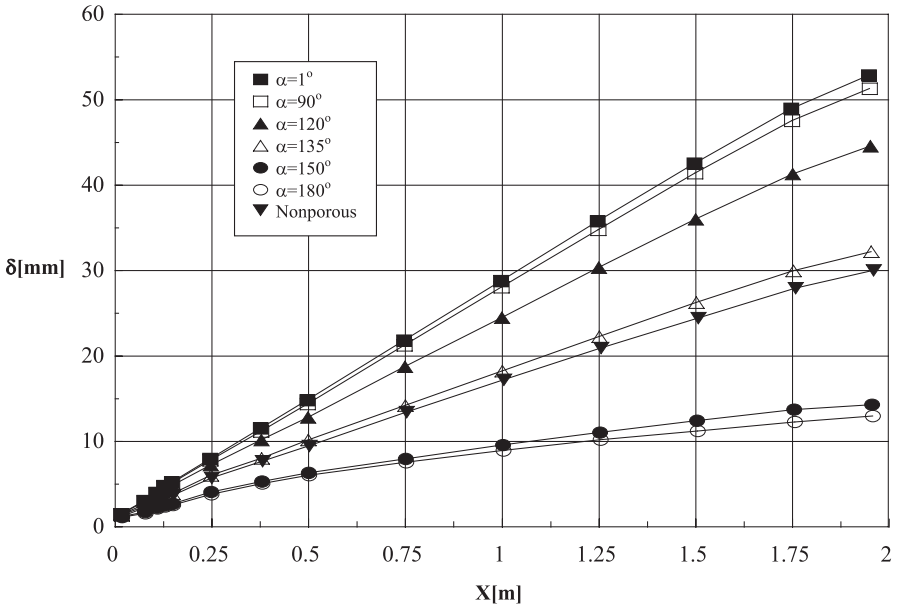

Figure 9.
Variation of the boundary layer thickness along the wall at different angles of injection for V_w = 0.004 m/s

Figure 11 indicates that the injection with the angles of $17^\circ \leq \alpha \leq 90^\circ$ causes the strongest adverse pressure gradients in the turbulent boundary layer. The effect of the angle of suction on the adverse pressure gradient is also seen in Figure 12.

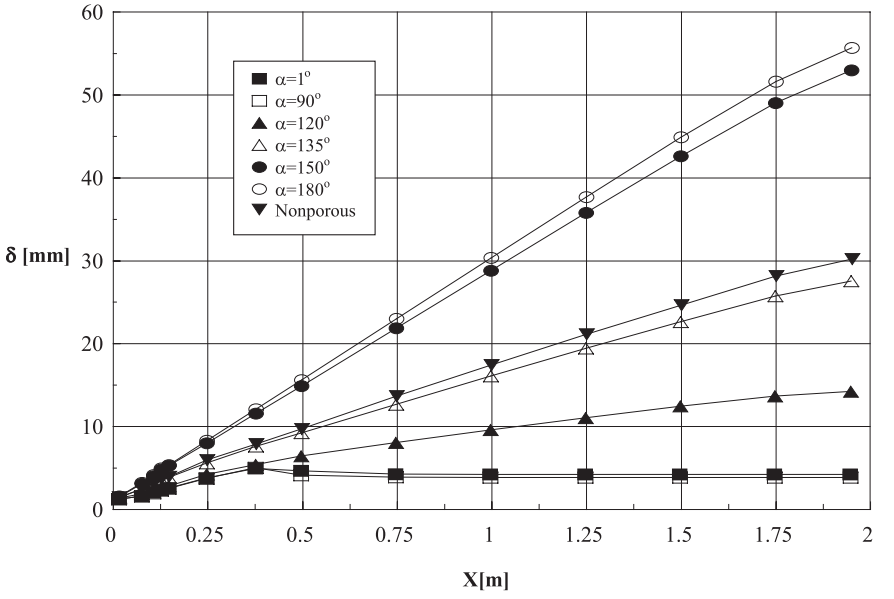

Figure 10.
Variation of the boundary layer thickness along the wall at different angles of suction for V_w = –0.005 m/s

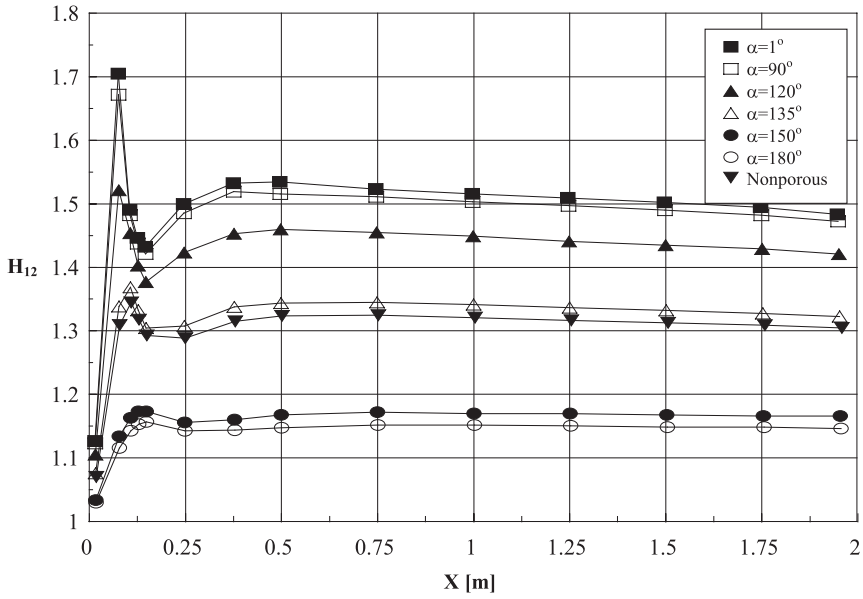

Figure 11.
Variation of the shape factor along the wall at different angles of injection for V_w = 0.004 m/s

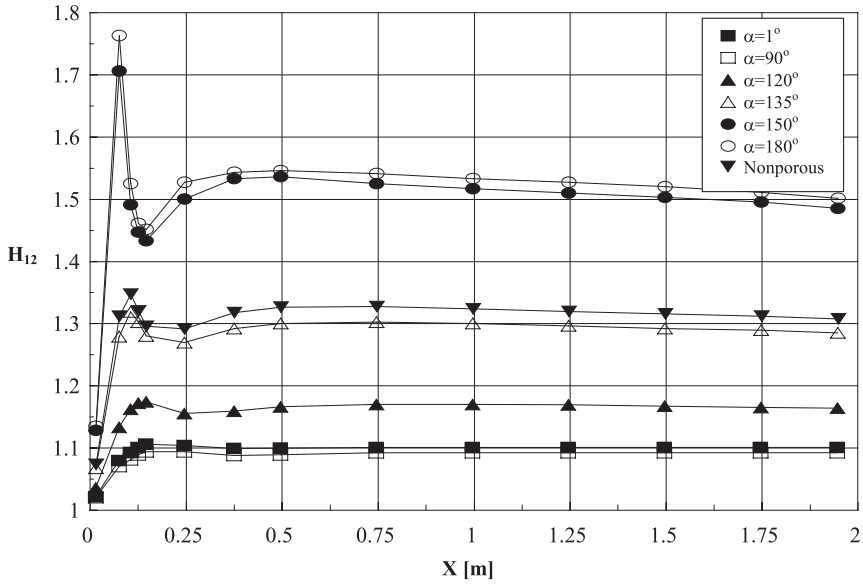

Figure 12.
Variation of the shape factor along the wall at different angles of suction for V_w = –0.005 m/s

Conclusions

The dimensionless velocity distribution in the turbulent boundary layer developing on a porous wall does not follow the universal velocity distribution law due to the effects of injection and suction. In a numerical simulation of the turbulent flow with mass transfer through porous wall, a special wall treatment is needed. For this reason, a modified wall function which includes the effects of

injection and suction should be used. As a method of controlling the boundary layer, the injection and suction through a porous wall can be successfully applied to control the drag and also to provide thermal protection at high velocities, with an adjustable angle of injection and suction.

References

Cebeci, T. and Bradshaw, P. (1977), *Momentum Transfer in Boundary Layers*, Hemisphere, Washington, DC.

Cebeci, T. and Smith, A.M.O. (1974), *Analysis of Turbulent Boundary Layers*, Academic Press, New York, NY.

Eckert, E.R.G. and Drake, R.M. (1972), *Analysis of Heat and Mass Transfer*, McGraw-Hill, New York, NY.

Hirt, C.W. and Cook, J.L. (1972), "Calculating three-dimensional flows around structures and over rough terrain", *J. Computational Physics*, Vol. 10, pp. 324-40.

Launder, B.E. and Spalding, D.B. (1979), *Mathematical Models of Turbulence*, Academic Press, London.

Patankar, S.V. (1980), *Numerical Heat Transfer and Fluid Flow*, Hemisphere, New York, NY.

Schetz, J.A. and Nerney, B. (1977), "Turbulent boundary layer with injection and surface roughness", *AIAA Journal*, Vol. 15, pp. 1288-93.

Schlichting, H. (1979), *Boundary-Layer Theory*, McGraw-Hill, New York, NY.

Simpson, R.L. (1970), "Characteristics of turbulent boundary layers at low Reynolds numbers with and without transpiration", *J. Fluid Mech.*, Vol. 42, pp. 769-802.

Yang, Y.T. and Kuo, C.L. (1997), "Numerical study of a backward-facing step with uniform normal mass bleed", *Int. J. Heat Mass Transfer*, Vol. 40, pp. 1677-86.

Yang, J.T., Tsai, B.B. and Tsai, G.L. (1994), "Separated-reattaching flow over a backstep with uniform normal mass bleed", *ASME J. Fluids Engineering*, Vol. 116, pp. 29-35.